



# Properties of Green, Lightweight, and High-Strength Reactive Powder Concrete Incorporating Modified Expanded Polystyrene Beads

Seyed Amin Azimi<sup>1</sup>; Ali Allahverdi<sup>2</sup>; and Mehdi Alibabaie<sup>3</sup>

Abstract: This work presents green lightweight reactive powder concrete (GLRPC) as a novel lightweight composite with improved properties by incorporating modified expanded polystyrene beads (MEPS) into green reactive powder concrete (RPC). It provides the advantages of both RPC and lightweight concrete (LWC). Because incorporation of the conventional expanded polystyrene (EPS) beads into the concrete mix results in a considerable loss of mechanical properties, it is necessary to find effective methods to preserve RPC properties as much as possible. The present work is devoted to the thermal modification of EPS. Various mixtures with different replacement levels of total RPC binder paste volume (0%, 15%, 30%, and 45%) with MEPS under different curing conditions (both standard water curing and heat curing conditions) were investigated in terms of their physical and mechanical properties. The results of the experimental study showed that MEPS beads had appropriate distribution into the GLRPC matrix without any considerable segregation. Replacement levels up to 30% of RPC paste volume by MEPS beads result in the development of high-strength lightweight concrete. Further replacement levels lead to lightweight concretes that drop into structural class. The water absorption shows a stronger dependency to curing temperature than replacement level of RPC paste volume with MEPS. The value of water absorption for all the studied mixtures, however, remained less than 2% that is relatively small. The microstructure analysis showed a very dense and uniform interfacial transition zone microstructure (ITZ) with good bonding of cement paste to MEPS beads. The relatively higher compressive strength of GLRPC cured at 200°C could be attributed not only to the development of a denser microstructure, but also to the development of hollow spherical polystyrene beads with hard and stiff shells resulting in an innovative high-tech plastic/cement-paste bonding. DOI: 10.1061/(ASCE)MT.1943-5533.0003995. © 2021 American Society of Civil E

Author keywords: Reactive powder concrete; Lightweight aggregate concrete; Expanded polystyrene (EPS); Efficiency factor.

### Introduction

Reactive powder concrete (RPC) is a relatively new kind of concrete, which can be considered among the latest concrete research innovations in concrete research due to its highly close-packed microstructure (Richard and Cheyrezy 1995; Yazıcı et al. 2010). According to the theoretical and practical points of view, a compact microstructure as a result of sufficient particle packing plays a very important role in achieving the outstanding mechanical properties and excellent durability performance of RPC (Bonneau et al. 2001; Cwirzen et al. 2008). The development of RPC is mainly attributed to several fundamental principles including, reduction of water-to-binder ratio (typically <0.18), elimination of coarse aggregates to achieve a particle size homogeneity, utilization of reactive siliceous

<sup>1</sup>Research Laboratory of Inorganic Chemical Process Technologies, School of Chemical Engineering, Iran Univ. of Science and Technology, Narmak, Tehran 1684613114, Iran. Email: AminAzimi114@gmail.com

<sup>3</sup>R&D Center of Robin EPC Company, Sa'adat Abad, Tehran 1981913651, Iran. Email: Mehdi\_alibabaie@yahoo.com

Note. This manuscript was submitted on December 10, 2020; approved on April 21, 2021; published online on September 30, 2021. Discussion period open until February 28, 2022; separate discussions must be submitted for individual papers. This paper is part of the *Journal of Materials in Civil Engineering*, © ASCE, ISSN 0899-1561.

materials to enhancing the SiO<sub>2</sub>-CaO ratio, incorporation of steel fibers to improving the ductility, application of presetting pressure to fresh concrete, and employment of postsetting heat treatment to modifies the microstructures (Gökçe et al. 2017; Richard and Cheyrezy 1995; Yazıcı et al. 2010).

In the last decades, researchers have focused on lightweight aggregate concrete (LWAC) as an important type of low density (<2,000 kg/m<sup>3</sup>) cement-based composite. The LWACs are initially produced by total or partial substitution of normal dense aggregates with specific low-density cellular aggregates (aggregates full of voids) (Costa et al. 2018; Sadrmomtazi et al. 2012). Because the weight of structures plays a vital role in their seismic stability, weight reduction is beneficial in increasing the stability of structures against seismic waves (Nikbin et al. 2018). Besides, highstrength LWACs, compared to normal weight concrete, represent an effective solution for the reduction in cross-sections of structural elements, a slight increase in free space, easy precast transportation, etc. Therefore, high-strength LWACs as a class of cost-effective and durable materials offer significant potential structural applications for offshore platforms, marine structures, high-rise buildings, longspan bridges, and act as a cost effect and durable structure (Nikbin et al. 2018; Sayadi et al. 2016; Shafigh et al. 2011). Nowadays, enhancing energy efficiency in buildings is considered as one of the most critical environmental issues in the construction industry. One reasonable method to reduce energy consumption and to enhance energy efficiency as well as protecting the ecological system is to improve the thermal properties of building materials (Ali et al. 2018; Chung et al. 2018; Maaroufi et al. 2018). The application

<sup>&</sup>lt;sup>2</sup>Professor, Research Laboratory of Inorganic Chemical Process Technologies, School of Chemical Engineering, Iran Univ. of Science and Technology, Narmak, Tehran 1684613114, Iran; Cement Research Center, Iran Univ. of Science and Technology, Narmak, Tehran 1684613114, Iran (corresponding author). ORCID: https://orcid.org/0000-0002-8988-9226. Email: ali.allahverdi@iust.ac.ir; ali.allahverdi@iust.ac.ir

of LWAC as a relatively new building material is a possible way to achieve this goal.

The unit mass of RPC is typically about 2,150–3,000 kg/m<sup>3</sup>, and the aggregates in its composition with a density often over 2,600 kg/m<sup>3</sup> are considered as high-density components. The silica fume used in the RPC composition has a density around 2,200 kg/m<sup>3</sup>. This significantly increases the structures dead load. As regards, the use of high amounts of lightweight aggregate can considerably reduce the unit mass of RPC. Sadrekarimi (2004) found that light-weight RPC with a density as low as 1,930 kg/m<sup>3</sup> and a compressive strength as high as 280 MPa, could be achieved with a high silica fume (SF) replacement and application of a high-temperature heat curing regime. Sadrekarimi noted that an increase in RPC's compressive strength due to incorporation of SF is through both pozzolanic and filling effect mechanisms. Gökçe et al. (2017) used pumice aggregate to produce lightweight RPC with densities between 1,840 and 2,430 kg/m<sup>3</sup> and compressive strengths varying in the range 69-176 MPa. In this study, compressive strength loss was prevented by applying both presetting pressures up to 50 MPa and autoclave curing regimes at temperatures as high as 270°C. The increased curing temperature was used to remove the microcracks created by load and unload of presetting pressure. In an attempt to find an effective solution for the reduction of the unit mass of RPC, recently Allahverdi et al. (2018) developed a green lightweight RPC by incorporating EPS beads as lightweight aggregate and also by total replacement of quartz powder with ground granulated blast furnace slag (GGBFS) for environmentally-friendly purposes. They reported compressive strengths between 20.8 and 85.6 MPa with densities varying from 1,257 to 1,840 kg/m<sup>3</sup>, respectively. Low mechanical strength of the EPS beads, loss of integrity, and inefficient compaction were considered essential factors resulting in loss of compressive

Expanded polystyrene (EPS) is classified as a thermoplastic hydrocarbon produced that can be produced from expandable polystyrene by utilization of steam or chemical treatment through high-temperature processes (Assaad and El Mir 2020; Milling et al. 2020; Sayadi et al. 2016). EPS can be considered a type of artificial LWA characterized by combinations of a low-density, nonabsorbent closed-cellular structure (consisting of 98% trapped airbubbles) with a hydrophobic nature (Assaad and El Mir 2020; Sayadi et al. 2016). It is extensively used in thermal and sound insulating composites, floor decks, cladding panels, curtain walls, offshore oil platforms, and floating marine structures (Assaad and El Mir 2020; Sadrmomtazi et al. 2012).

Many research works have been devoted to Portland cement-based composites incorporating EPS as LWA to reduce the weight for structural and nonstructural purposes (Allahverdi et al. 2018; Babu and Babu 2003; Sadrmomtazi et al. 2012; Sayadi et al. 2016). Some studies were mainly concentrated on the characterization of thermal and mechanical properties as well as assessing its durability (Sadrmomtazi et al. 2012; Sayadi et al. 2016). Published results, however, indicate that incorporation of EPS into concrete weakens its properties, mostly mechanical properties. In other words, cement-based composites associated with EPS lightweight concrete have demonstrated a meager strength range, which makes it unsuitable for actual engineering.

Following our recent study (Allahverdi et al. 2018) on the incorporation of EPS beads as a lightweight aggregate to develop GLRPC, here in this study, the focus is on the improvement of properties of EPS for achieving the following four main objectives: (1) improving the uniform distribution of LWA into RPC matrix and reducing segregation tendency; (2) converting EPS into a high-strength load-bearing plastic aggregate by densifying its soft

structure; (3) improving the bonding tendency between GLPRC paste and plastic aggregate; and (4) converting MEPS beads inside the GLRPC matrix into hollow spherical polystyrene beads with innovative high-tech plastic/cement-paste bonding. In summary, the present study is aimed at eliminating or at least reducing the disadvantages of EPS beads inside the GLRPC to expand its applications with acceptable properties. The soft and weak structure of EPS beads was modified into a tight structure through heat treatment in an electric oven at about 150°C, according to Kan and Demirboğa's (2008) method. To assess the effect of MEPS beads on the mechanical and physical properties of RPC, an accurate experimental plan was implemented. The image analysis method has been employed to evaluate the MEPS distribution in the paste. Various physical and mechanical properties include compressive strength under different curing conditions, efficiency factor, and water absorption, were investigated. The microstructure of the GLRPCs cured at different curing conditions was studied with scanning electron microscope (SEM).

# **Experimental Design**

#### Materials

Type II portland cement, CEM-II (PC) 42.5 R, in accordance with ASTM C150 (ASTM 2017) used in this work, was supplied by Tehran Cement Company located in Tehran, Iran. Undensified silica fume with a maximum SiO<sub>2</sub> content of about 96% complying with ASTM C1240 (ASTM 2005) was prepared from Iranian ferroalloys industries (Lorestan, Iran). GGBFS supplied by the Isfahan Steel (Isfahan, Iran) Company was used as a total replacement material for quartz powder and quartz sand because of the following reasons: (1) the recycling of high volumes of an industrial waste as a concrete additive; (2) preventing the depletion of the natural resources; and (3) improving MEPS adhesion to cement paste. RPC is classified as a high-quality special type of concrete with specific applications that exhibits exceptional durability and high mechanical properties. These interesting properties can be achieved by consumption of high amount of cement (between 800 and 1,000 kg/m<sup>3</sup>) and active powders. The environmental advantages of RPC developed in the present study are compared to other types of RPCs and not to conventional concrete. Also, the green promise in the present study is related to RPC paste in which quartz powder was completely substituted by GGBFS and MEPS aggregate as an inert substance only contribute to decrease the weight of the composite. Knowing that in the concrete industry after Portland cement, utilization of aggregate is known as the primary source of CO2 emission, which corresponds to 13%–20% of the total  $CO_2$  emissions (Shafigh et al. 2013). In conventional RPC, the aggregate share in CO2 emission is much more announced due to the necessary energy-intensive grinding process of quartz that is highly abrasive. Due to the limitations of natural resources, partial replacement of the aggregate with waste and recycled materials is the key to prevent the destruction of resources and may be one of the better solutions for energy conservation in structural applications (Gupta et al. 2014; Shafigh et al. 2013). The chemical and physical properties, as well as the grading curves of the basic components (cement, silica fume, and GGBFS), are given in Tables 1 and 2, and Fig. 1, respectively. A superplasticizer (SP) based on polycarboxylate, in conformity with ASTM C494 (ASTM 2013a), was employed.

Commercial grade EPS beads with particle sizes between 2.61–5.56 mm were modified and used as lightweight artificial aggregate. The modification process based on heat treatment aimed at changing the soft structure of EPS into a tight structure of improved

Table 1. Chemical compositions of cement, silica fume, and GGBFS

Composition	CaO	$SiO_2$	$Al_2O_3$	$Fe_2O_3$	MgO	$K_2O$	$SO_3$	$TiO_2$	LOI
Cement	63.26	22.5	4.15	3.44	3.25	0.65	1.80	_	0.61
Silica fume	0.35	96.12	0.82	0.59	0.29	0.40	0.10	_	0.63
GGBFS	36.91	36.06	9.16	0.70	10.21	0.70	1.15	3.5	_

**Table 2.** Physical properties of cement, silica fume, and GGBFS

Physical properties	Density (kg/m <sup>3</sup> )	Specific surface area (m²/kg)	Color
Cement	3,150	302	Green
Silica fume	2,130	18,000	Gray
GGBFS	2,600	320	Beige

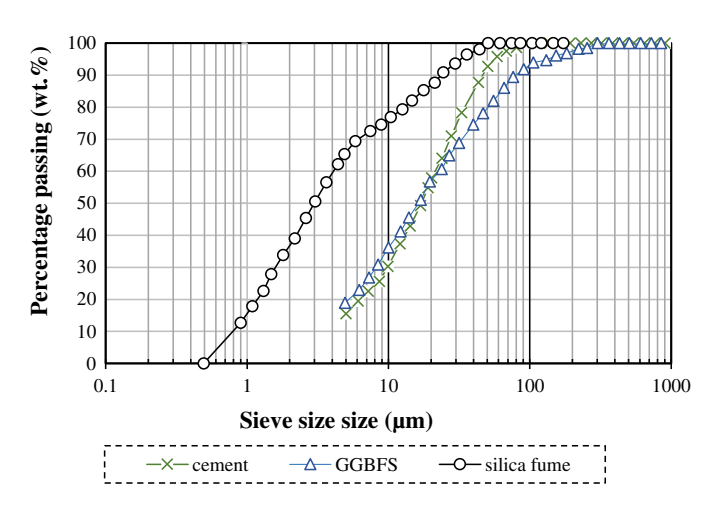


Fig. 1. Granulometric curves of cement, silica fume, and GGBFS.

mechanical properties through controlled shrinkage. For this, the EPS beads were placed in an electric oven at about 150°C for 5 min and afterward allowed to cool down at ambient temperature. When EPS beads are heated at a temperature in the range of 110°C-150°C, they undergo a structural collapse leading to significant shrinkage, volume reduction, and a significant increase in mechanical properties. At 160°C, polystyrene beads melt and a viscous residue is formed (Kan and Demirboğa 2008; Mehta et al. 1995; Miskolczi et al. 2006). Fig. 2 demonstrates the schematic of the EPS beads modification process adopted from the Kan and Demirboğa (2008) method with slight modifications. The transformation of EPS bead microstructure is clearly illustrated in SE microphotographs displayed in Fig. 3. The test results displayed significant changes in density, particle size distribution, and mechanical strength, which are summarized in Table 3 and Fig. 4. Two-dimensional (2D) image analyses were performed to achieve a particle size distribution curve for EPS and MEPS. During image processing, agglomerated aggregates were detached according to the Han et al. (2016) method.

# Mix Design

The properties of lightweight concretes are remarkably influenced by three main groups of parameters, including: (1) content and composition of the binder; (2) LWA properties including density,





Fig. 2. Illustration of EPS beads: (a) before heat treatment; and (b) after heat treatment

strength, porosity, texture, and surface roughness; and (3) curing conditions. Because simultaneous examination of multiple influencing variables is costly and needs a lot of time, the present study is limited to the effect of replacement level of RPC paste volume with MEPS and curing conditions, considering all the influencing factors constant. Therefore the mixture designs used in this work were similar to our previous work on GLRPC (Allahverdi et al. 2018). Accordingly, the proportioning of cement, SF, GGBFS, water was equal to 1:0.24:1. 32:0.297. In all mixtures, the water/ (PC + SF) ratio was maintained at 0.24 for ensuring full compaction and adequate workability as well as a high degree of hydration. Moreover, the SF/PC ratio was fixed at 0.24 to achieve a value of 1.3 for the molar ratio of CaO/SiO<sub>2</sub>, which is proposed as an optimum value by Yazıcı et al. (2008). The study conducted by Kan and Demirboğa (2008) reports the details of EPS properties modified thermally at different temperature and time conditions. Therefore, appropriate thermal modification conditions were selected according to their study. In order to investigate the effects of MEPS content on basic engineering properties of GLRPC, LWA were used at replacement levels of 0% (as control), 15%, 30%, and 45% by volume of RPC binder paste corresponding to unit mass reductions equivalent to 0, 57.4, 115.2, and 172.2 kg/m<sup>3</sup>, respectively. For simplicity, GLRPC mixtures were named GM-X, in which X represents the percentage of replacement by volume. The mix proportions of GLRPC mixtures are given in Table 4.

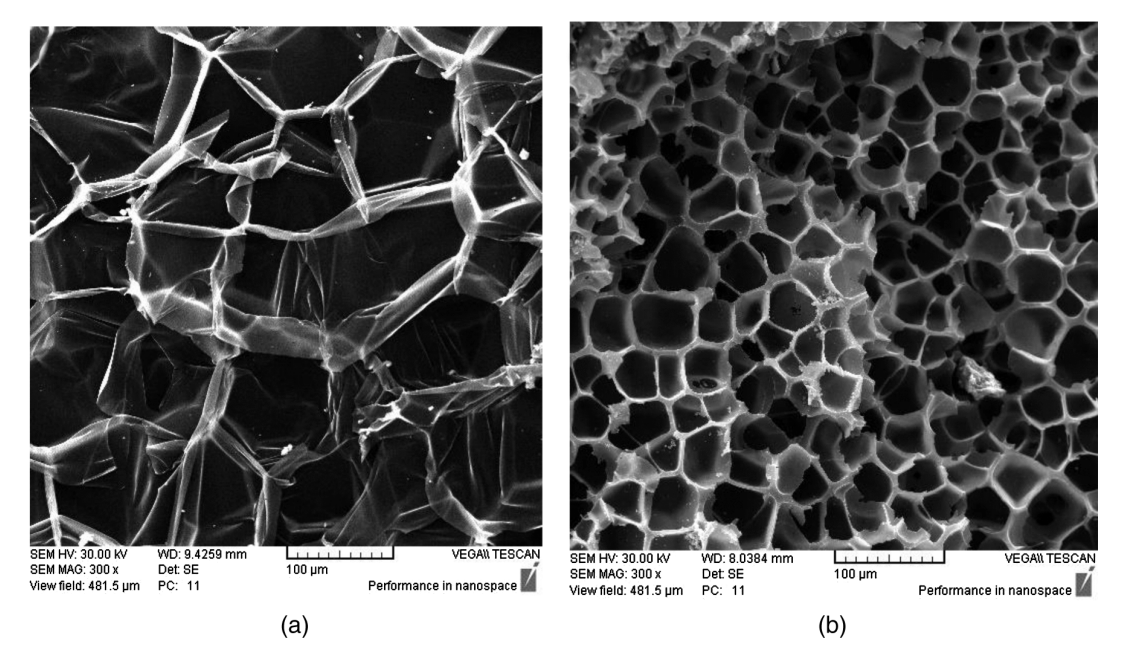


Fig. 3. SEM microphotographs: (a) EPS microstructure; and (b) MEPS microstructure.

Table 3. MEPS and EPS beads properties

Property	Density (kg/m <sup>3</sup> )	Melting point (°C)	Volatilization point (°C)	Strength (MPa)	Maximum diameter (mm)	Average diameter (mm)	Water absorption (% by weight)
MEPS	330	160	450–500	~8	2.36	~1.6	~0
EPS	16	160	450–500	Negligible	5.56	~4.42	~0

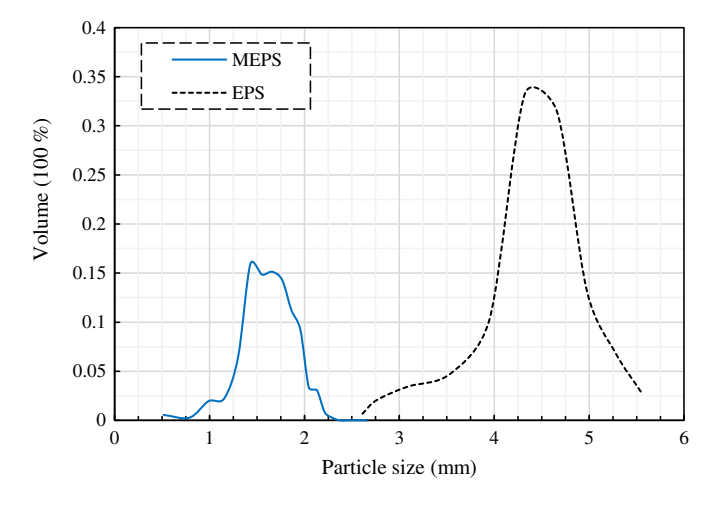


Fig. 4. Particle size distribution curves for EPS and MEPS.

**Table 4.** Mix proportions of GLRPC (kg/m<sup>3</sup>)

Mix	В	inder				MEPS
code	PC	SF	GGBFS	W/(PC+SF)	SP	beads
GM-0	793	190.32	1,046.76	0.24	23.79	0
GM-15	675	162	891	0.24	20.25	57.4
GM-30	554	132.96	731.28	0.24	16.62	115.2
GM-45	436	104.64	575.52	0.24	13.08	172.2

# Preparation, Curing, and Testing

The GLRPC mixing details were as follows: (1) the dry components of the binder (PC, SF, and GGBFS) were mixed in an epicyclic mixer at its low speed (140 rpm) for about 3 min; (2) half of the water premixed with SP was added to the dry componentcomposition, and mixing was continued at a higher speed (285 rpm) for a further 3 min; (3) the other half of the water premixed with SP was added to the mixture with continued mixing at the same higher speed for about 10 min to obtain a plastic consistency; (4) the mixing speed was changed to low speed and the MEPS beads were added to the mixture and mixing was continued for 3 min to achieve uniform distribution of MEPS beads; and (5) the fresh GLRPCs were then cast into oiled molds of two different sizes  $(5 \times 5 \times 5 \text{ cm} \text{ and } 10 \times 10 \times 10 \text{ cm})$  and compacted by hand in order to minimize the segregation of beads. The molds were then placed in a humid chamber at  $23.0^{\circ}\text{C} \pm 2.0^{\circ}\text{C}$  and  $95\% \pm 3\%$ relative humidity for 24 h. Then, that the GLRPC cubes were demolded and divided into four groups and each group underwent a different curing regime, including: (1) standard 28-day water curing at 23.0°C  $\pm$  2.0°C; (2) 4 days of standard water curing at 23.0°C  $\pm$ 2.0°C followed by 48 h of heat curing in an oven at 100°C  $\pm$  1°C; (3) 4 days of standard water curing at  $23.0^{\circ}\text{C} \pm 2.0^{\circ}\text{C}$  followed by 48 h of heat curing in an oven at 150°C  $\pm$  1°C; and (4) 4 days of standard water curing at  $23.0^{\circ}\text{C} \pm 2.0^{\circ}\text{C}$  followed by 48 h of heat curing in an oven at  $200^{\circ}\text{C} \pm 1^{\circ}\text{C}$ .

A hydraulic compression-testing machine (SCL brand) with  $\pm 1\%$  accuracy and a capacity of 3,000 kN was used for compressive strength tests at a loading rate of 0.25  $\pm$  0.05 MPa/s, in accordance with ASTM C109 standard (ASTM 2012). Three 5  $\times$  5  $\times$  5 cm

cube specimens were employed for each measurement. To measure MEPS distribution in GLRPC matrix, a 2D image analysis method was employed. The GLRPC cubes of the size  $5 \times 5 \times 5$  cm were cut into halves to expose cross-sections, and image analysis was carried out using imageJ version 1.44P software. Microstructural analyses were performed using a TESCAN VEGA II (Czech Republic) SEM using secondary electron image (SE) mode at 30 kV. For this, thin slices were prepared from selected samples. These slices were then dried and coated with a thin gold layer prior to imaging.

Water absorption tests complying with ASTM C642-13 (ASTM 2013b) were performed on  $10 \times 10 \times 10$ -cm GLRPC cubes using Eq. (1). For this, the GLRPC cubes were first placed in water with a temperature-controlled at 21°C for 72 h and after measuring their water-saturated masses, they were oven-dried until they reached a constant oven dry mass to be measured

Water absorption(%) = 
$$[(SM - ODM)/ODM] \times 100$$
 (1)

where SM = saturated mass; and ODM = oven-dry mass.

## **Results and Discussion**

# Dispersion of MEPS

The incorporation of EPS beads into a cement paste may lead to the appearance of rich and poor regions. Inappropriate distribution of EPS in cement paste matrix can occur due to the floating tendency of EPS beads in fresh cement paste resulting from low density and hydrophobic nature of EPS (Wu and Sun 2007). In this regard, a 2D-image analysis method has been employed in this work to evaluate MEPS distribution in cement paste by analyzing the photographed cut-surface of specimens with imageJ version 1.44 software. This was implemented in four main steps, including: (1) specimens were cut into halves to obtain cross-section surfaces; (2) the cut surfaces were photographed; (3) the photographs were rotated 90° clockwise for the accurate evaluation of floating phenomenon in the composite; and (4) finally, image analysis was performed for evaluating MEPS distribution inside cement paste matrix based on a binary operation, which allowed accurate recognition of different phases using the black and white colors for MEPS and cement paste, respectively.

The MEPS distribution analysis was performed on specimens of three mixtures including; GM-15, GM-30, and GM-45, as shown in Fig. 5. The corresponding binary images of the same three specimens from left to the right with specimens' top surfaces at the casting time rotated to the right side are shown in Fig. 6. As seen, MEPS beads represent a relatively uniform distribution inside the cement paste matrix, and there is no region of low or high density. Furthermore, the method used by Allahverdi et al. (2018) in that the variation of the number of beads (NOB) and gray value (GV) (the surface area in pixel scale for EPS beads on the cut surface of the specimen) along the casting direction was used for quantitative examination of distribution homogeneity of MEPS inside the cement paste matrix. The changes in GV along casting direction (from bottom to the top surface of the specimens) are shown in Fig. 7, in which the diagrams show an almost constant GV across all the specimens. This means that MEPS beads distribution inside all three specimens shows a relative uniformity in terms of the beads' surface area.

Variations in NOB across the cut-surfaces of the specimens from bottom to top are displayed in Fig. 8. As seen, NOB varies in limited intervals between 20-40, 50-70, and 64-73 for the specimens GM-15, GM-30, and GM-45, respectively. To determine the degree of segregation, straight lines with the best fit to the NOB are plotted. As seen, all three lines are less steep with small slopes, either positive or negative, showing no correlation with replacement level. Compared to GLRPC with EPS beads (Allahverdi et al. 2018), GLRPC made with MEPS beads has the highest level of homogeneity and appropriate distribution. Surface modifications including increased roughness and density increase in MEPS due to thermal treatment are among the significant factors causing this distribution uniformity within the cement paste matrix. Therefore, the thermal modification of EPS beads satisfactorily prevents the phenomenon of floating and segregation that are among the major problems of incorporating EPS beads into the cement paste. Hitherto modifying additives and supplementary cementitious materials (SCMs) have been used as appropriate solutions to improve EPS beads distribution in cement paste matrix (Wu and Sun 2007). Applying SF along with SP (Babu and Babu 2003), researchers attempted to improve the hydrophobicity of EPS beads and increase EPS bonding with cement paste in order to minimize segregation and increase cohesiveness with the matrix.

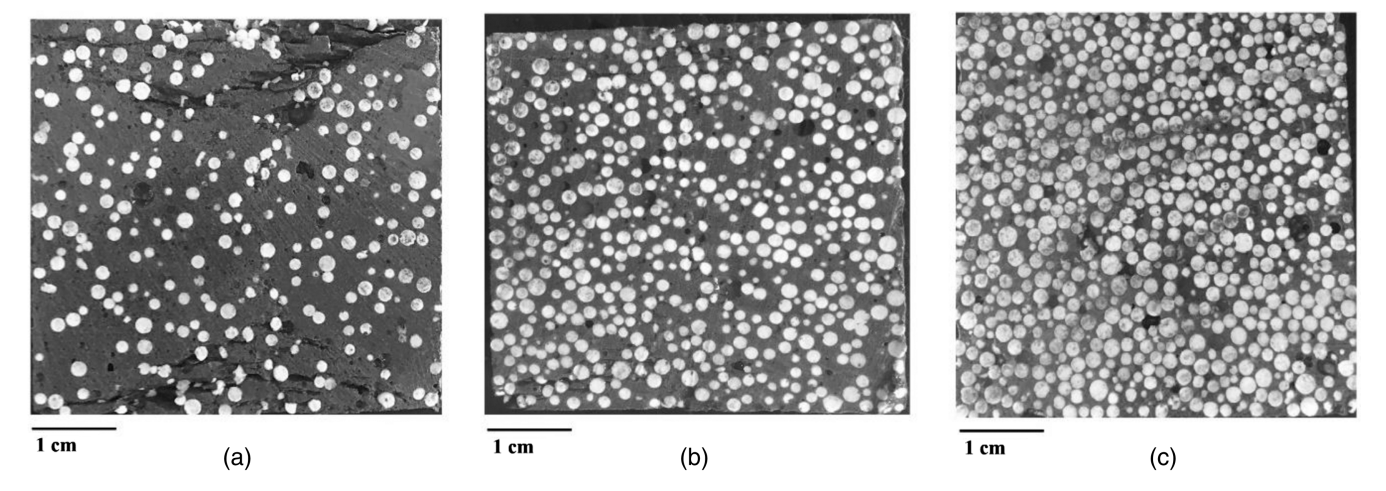


Fig. 5. Section images of analyzed specimens: (a) GM-15; (b) GM-30; and (c) GM-45 (top surfaces of the specimens at the time of casting were positioned on the right side).

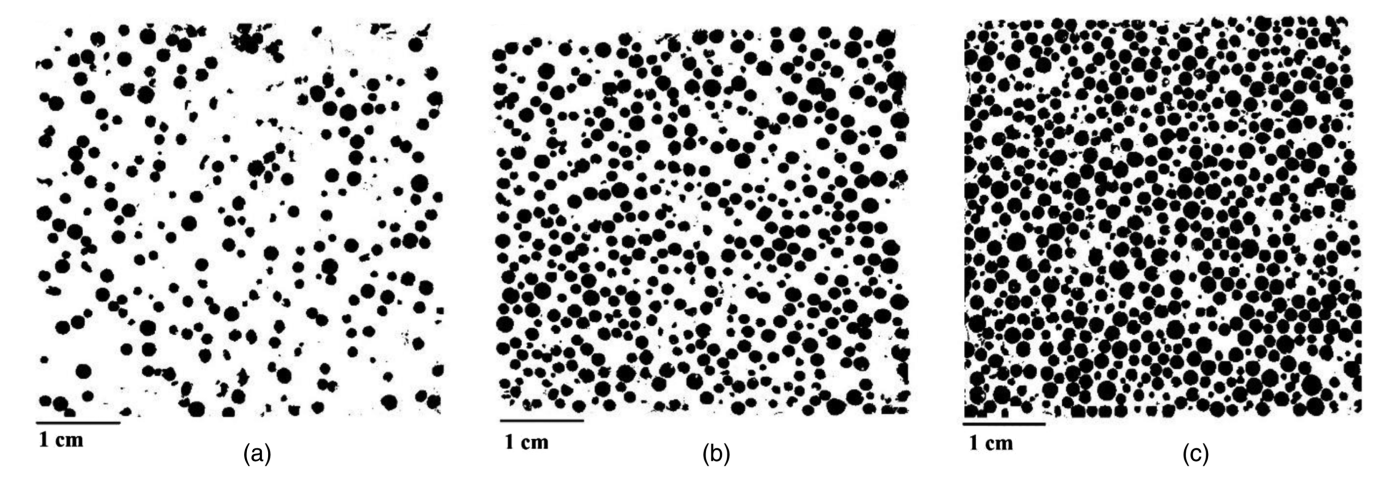


Fig. 6. Binary images of specimens: (a) GM-15; (b) GM-30; and (c) GM-45 (top surfaces of the specimens at the time of casting were positioned on the right side).

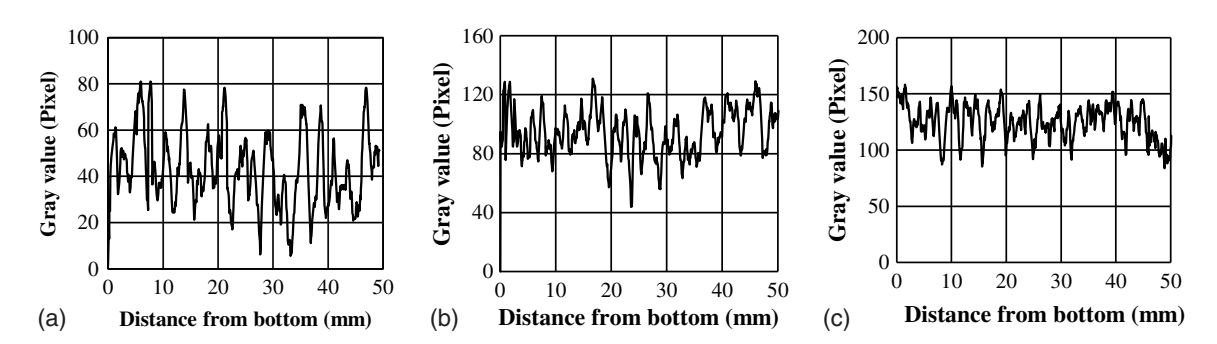


Fig. 7. Relationship between gray value and distance from bottom to top for specimens: (a) GM-15; (b) GM-30; and (c) GM-45.

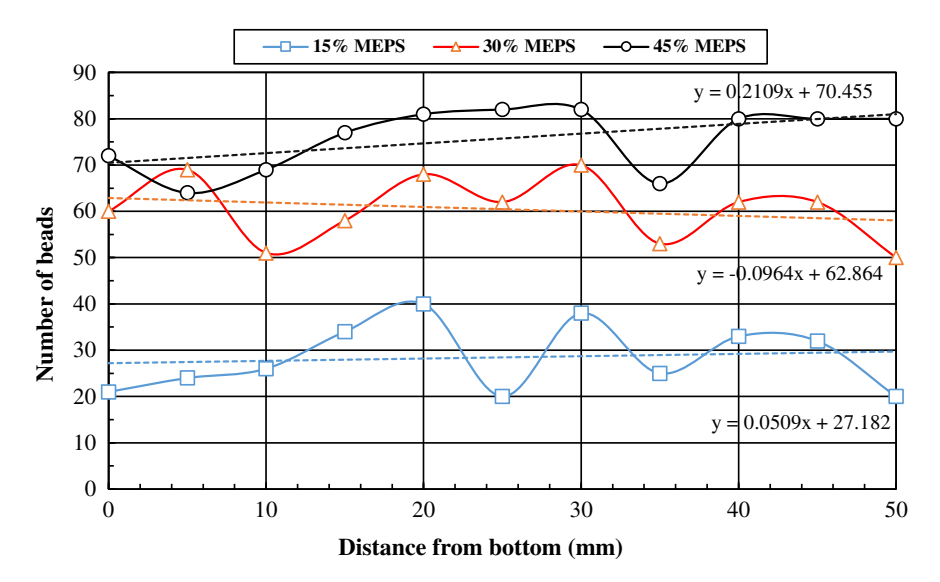


Fig. 8. Relationship between number of beads and distance from bottom to top for specimens GM-15, GM-30, and GM-45.

# Compressive Strength

#### Influence of Replacement Level and Curing

Fig. 9 shows the compressive strength variations of GM-0, GM-15, GM-30, and GM-45 at different ages (3, 7, 28, and 56 days) of

standard water curing. As seen, compressive strength varies significantly depending on the substitution level and curing age. The compressive strength tends to decrease with the incorporation of MEPS enormously. The higher the replacement level, the higher the strength loss. Compared to GM-0, as control mix, specimens

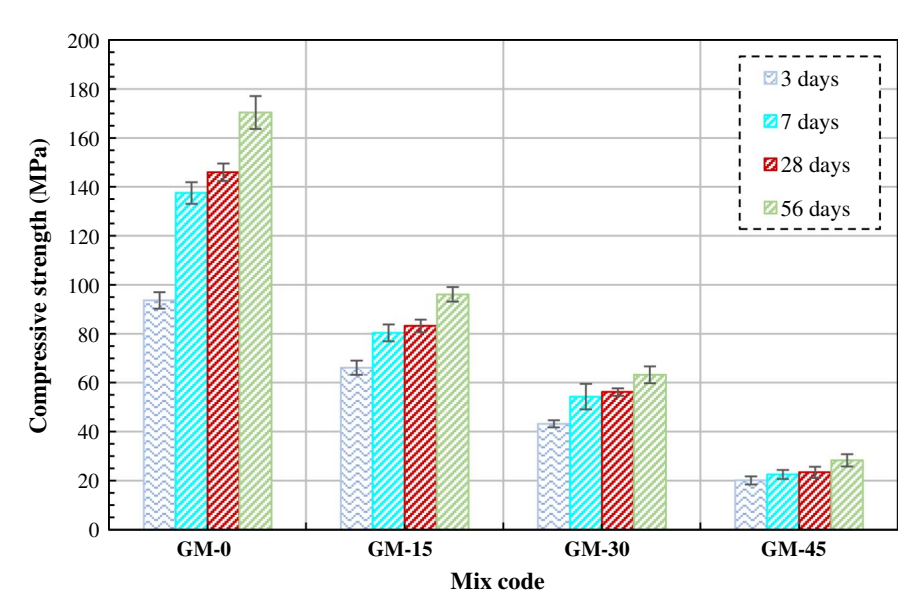


Fig. 9. Compressive strength of different GLRPC specimens at different ages of standard water curing.

of mixes GM-15, GM-30, and GM-45 show strength losses of about 43%, 61%, and 84%, which are equivalent to 63, 90, and 123 MPa after 28 days of standard water curing, respectively. EPS and MEPS, compared to natural aggregate, have very porous, soft structures, lower strength, high compressibility behavior, and the incorporation of which into the mix weakens the concrete properties, mainly mechanical, by merely increasing the less stiffness material content of the concrete (Gupta et al. 2014; Sayadi et al. 2016). Also, elimination of coarse aggregate with a maximum limiting size of 650  $\mu$ m and achievement of a close-packing state through aggregate grading optimization is known as a critical feature in conventional RPC mixtures (Aydin et al. 2010; Bonneau et al. 2001; Cwirzen et al. 2008). The dramatic compressive strength loss of RPC due to incorporation of EPS or MEPS can be attributed to the relatively large aggregate size (about 1.55 mm in the present work) exceeding the recommended limiting size, in addition to the physical nature of the MEPS (i.e., porous and soft texture).

Additionally, the amount of entrapped air voids of concrete is one of the crucial parameters that influence the concrete strength. As a practical example, the results from the air-entrained concrete investigation indicated that increasing the amount of entrained air up to 8% causes a reduction in compressive strength of about 45%. Here, the incorporation of MEPS beads, due to the hydrophobic nature of these materials, increases the entrapped air voids (extra porosity) of RPC that could contribute to considerable strength loss (Khaloo et al. 2008; Neville 1995). In a different research work on concrete incorporating waste rubber tire as fine aggregate (Gupta et al. 2014), the loss in compressive strength of lightweight concrete was attributed to the porosity increase due to air-entraining caused by rubber aggregate. This air-entraining could occur either as entrapped air bubbles and/or probably enlarged ITZ, which is regarded as an important parameter controlling the concrete mechanical properties (Yanzhou et al. 2015). Because there is no or weak interaction between organic aggregates (like shredded PET, plastic waste, MEPS beads,. etc) and cement hydrate as an inorganic material, the incorporation of MEPS beads into concrete can result in an enlarged and more porous ITZ (Saikia and Brito 2012; Saikia and De Brito 2014).

Another important observation from Fig. 9 is the effect of MEPS on the rate of strength development. As seen, the rate of strength

development of GLRPC significantly depends on the MEPS content of the matrix, so that increasing the MEPS content leads to the lower rate of strength development. This behavior in mixtures of higher density can be related to the silica fume pozzolanic reaction with Ca(OH)<sub>2</sub>, which progresses with curing age (Richard and Cheyrezy 1995; Zanni et al. 1996). Another reason for this observation is the difference in hydraulic properties of GGBFS and portland cement. GGBFS shows significantly slower initial hydration reaction rate than cement and displays superlative strengths at later ages especially later than 40 days (Cheah et al. 2019; Ganesh and Murthy 2019; Yazıcı et al. 2010). This hydraulic behavior of GGBFS compared to portland cement results in significant strength development evident in the standard water-cured samples at the age of 56 days compared to the age of 28 days (Majhi et al. 2018).

#### **Influence of Curing Temperature**

Fig. 10 represents compressive strength variations of GLRPC mixtures with different MEPS contents under both 28-day standard water curing and 48 h of heat curing at different temperatures of 100°C, 150°C, and 200°C after 4 days of curing at standard water curing conditions. As expected, the value of compressive strength of all the mixtures displayed a more significant increase, when the heat curing temperature was increased, except heat curing at 100°C that showed a slight decrease in compressive strength even in comparison with 28-day standard water curing conditions. Heat curing conditions at 200°C resulted in about 21%, 31%, 31%, and 40% increase in compressive strength of mixtures with replacement levels of 0%, 15%, 30%, and 45%, respectively, compared to corresponding mixtures cured for 28 days of standard water curing. Variations of compressive strength in a given mix design due to changes in curing conditions is attributed to the degree of hydration. This is discussed in detail in our previous publication (Allahverdi et al. 2018). Increasing curing temperature could effectively enhance the C-S-H chain length during the progress of hydration reactions of cement, in addition to its significant effects on both rate and degree of progress of pozzolanic reactions between calcium hydroxide and mineral admixture present in the cementitious system of RPC (Richard and Cheyrezy 1995; Tam et al. 2010; Zanni et al. 1996). In fact, part of GGBFS and SF as reactive materials remain unreacted under standard water curing conditions at room temperature and this unreacted part plays just a space-filling

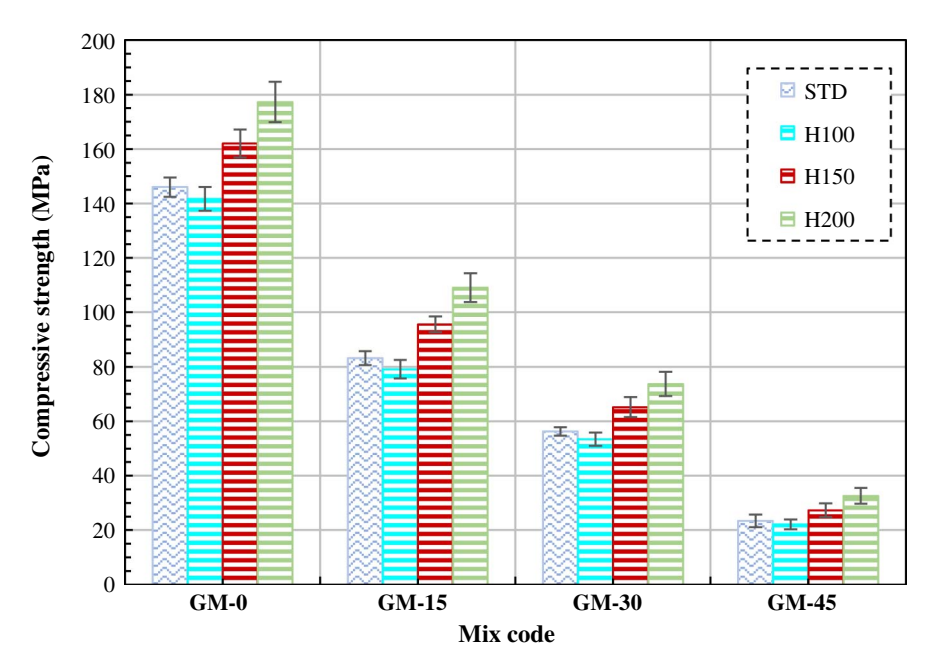
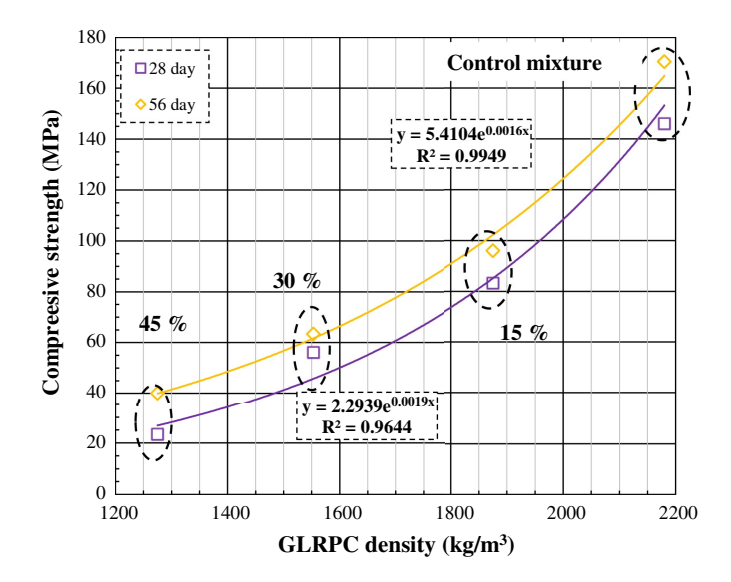


Fig. 10. Effect of heat curing application on compressive strength (where STD = 28-day standard curing; H100 = heat curing at 100°C; H150 = heat curing at 150°C; and H200 = heat curing at 200°C).

role in the RPC matrix. High-temperature curing facilitates the progress of secondary hydration reactions developing more calcium silicate hydrate (C-S-H) as well as the compressive strength (Vigneshwari et al. 2018; Yazıcı et al. 2010; Zanni et al. 1996). Furthermore, high temperature curing can improve and densify the microstructure of RPC through formation of crystalline C-S-H hydrates. Heat treatment changes the chemistry of hydration products by reducing CaO/SiO<sub>2</sub> ratio and the H<sub>2</sub>O/CaO ratio (Hiremath and Yaragal 2017; Yazıcı et al. 2008, 2010). At temperatures between 100°C and 150°C, C-S-H forms but started to convert to tobermorite with chemical formula Ca<sub>5</sub>Si<sub>6</sub>O<sub>16</sub>(OH)<sub>2</sub>, 4H<sub>2</sub>O, or C<sub>5</sub>S<sub>6</sub>H<sub>5</sub>. Tobermorite crystals have a stable chemical composition with an approximately CaO/SiO<sub>2</sub>-0.83 molar ratio and a hardness of 2.5 on the Mohs scale that combine to form a compact lattice, leading to higher compressive strength. At higher heat treatment temperatures between 150°C and 200°C secondary xonotlite are detected. The xonotlite crystals (Ca<sub>6</sub>Si<sub>6</sub>O<sub>17</sub>(OH)<sub>2</sub>) are triple chain silicate with an approximate CaO/SiO<sub>2</sub>-1 molar ratio and appear to be interlocking fibrous or acicular in shape (Hiremath and Yaragal 2017; Shen et al. 2019; Xun et al. 2020; Yazıcı et al. 2008, 2010). It is claimed that formation of C-S-H crystals (tobermorite and xonotlite) in RPC microstructure plays a significant role in strength development of RPC when compared with RPC without crystalline calcium silicate phases (Hiremath and Yaragal 2017; Shen et al. 2019; Xun et al. 2020).

# Relationship between Compressive Strength and Density

Fig. 11 represents the relationship between the 28-day and 56-day compressive strengths with dry density of concrete. As seen, compressive strength decreases exponentially with decreases in the concrete density, similar to the previous study (Allahverdi et al. 2018). The results indicated that the densities of GLRPCs incorporating MEPS beads (1,875–1,275 kg/m³) were about 14%–41.5% lower than the density of the control mixture (2,180 kg/m³). Comparing the achieved results with ACI 213, the 28-day compressive strengths of GM-15 (83.2 MPa) and GM-30 (56.2 MPa) are much higher than the specified minimum compressive strengths for high-strength lightweight concrete (40 MPa or greater) and the



**Fig. 11.** 28- and 56-day compressive strengths of the GLRPC specimens versus density.

lightweight structural concrete concrete (17 MPa or greater). Furthermore, the 28-day compressive strength of GM-45 (23.4 MPa) meets the minimum 28-day compressive strength specified for lightweight structural concrete. Based on the experimental results, 28- and 56-day compressive strengths versus dry density of GLRPC can be computed using Eqs. (2) and (3)

$$F_{28C} = 2.2939 \times \exp(0.0019 \times D) \tag{2}$$

$$F_{56C} = 5.4104 \times \exp(0.0016 \times D) \tag{3}$$

where  $F_{28C}$ ,  $F_{56C}$ , and D = compressive strength (MPa) and the dry density (kg/m<sup>3</sup>) of the composite, respectively.

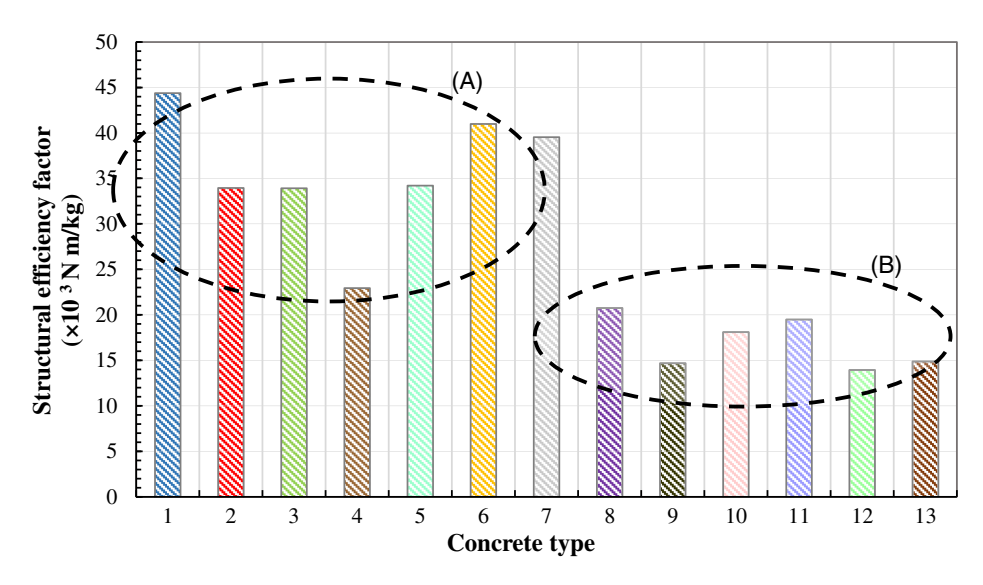


**Fig. 12.** Structural efficiency for different lightweight concrete specimens: (a) high-strength lightweight concrete class; and (b) structural lightweight concrete class. Note: 1 = present study; 2 = EPS; 3 = expanded glass (Rumsys et al. 2018); 4 = oil palm shell and oil palm boiler cliker (Aslam et al. 2017); 5 = expanded clay (Rumsys et al. 2018); 6 = expanded shale ceramist (Wu et al. 2019b); 7 = pumic (Gökçe et al. 2017); 8 = polypropylene (Záleská et al. 2018); 9 = apricot shell (Wu et al. 2018); 10 = rubber & expanded clay (Angelin et al. 2020); 11 = pumic (Demirel et al. 2019); 12 = carpet waste (Fashandi et al. 2020); and 13 = peach shell (Wu et al. 2019a).

The beneficial impact of the concrete weight reduction on building applications has been proven. GLRPC provides an interesting solution for construction cost-effectiveness, better thermal insulation, better fire insulation, slimmer structural elements, earthquake resistance, higher durability, and even easy transportation and installation operation. Moreover, with the development of high strength LWC technology, due to its significantly lower unit weight compared to normal concrete, construction of some impressive structures, like greater bridge spans, large domes, high building in weak soils, etc., has become possible, that was impossible or already constraint (Ali et al. 2018; Sayadi et al. 2016).

# Efficiency Factor

LWAC has served as an essential material for structural purposes in recent decades. For lightweight structural concretes, density and strength are important characteristics. Mostly when used in the offshore applications, bridges, and large high-rise buildings, a decreased in density while retaining strength is crucial (Chung et al. 2018; Rossignolo and Agnesini 2002; Yu et al. 2013). The correlation between strength and density of lightweight concrete is expressed through the structural efficiency factor. In other words, this factor provides an appropriate evaluation for performance characterization of different lightweight concretes, and can be written as follows:

$$EF = \frac{\sigma}{\rho}$$

where EF,  $\sigma$ , and,  $\rho$  = structural efficiency (N · m/kg); 28-day compressive strength (N/mm<sup>2</sup>); and dry density of concrete (kg/m<sup>3</sup>), respectively.

The structural efficiency of the GM-15 mixture developed in this work and some other lightweight concrete developed by other researchers with an oven-dry density of 1,800–1,900 kg/m³ and containing different types of LWA in two distinct classes, including the structural lightweight and high-strength lightweight concrete are determined and represented in Fig. 12. As seen, the structural

efficiency factor of the GM-15 mix with a value close to 45,000 N  $\cdot$  m/kg is much higher than structural efficiency factors of all LWACs in the structural lightweight concrete class. This is because of the compressive strength of mix GM-15 that is much higher (by about 100%-260%) than the reported compressive strengths for LWACs in the structural lightweight concrete class with the same oven-dry density. Also, compared to all LWACs in the high-strength lightweight concrete class, GM-15 exhibits a higher structural efficiency factor by about 4%-100%.

It is interesting to compare the structural efficiency factor of mix GM-15 with similar mix No. 2 in high-strength lightweight concrete class, which was developed in the authors' previous work (Allahverdi et al. 2018) using the same green RPC, the same mix design, and the same curing conditions except than using EPS instead of MEPS. Mix GM-15 has a structural efficiency factor 44% higher than mix No. 2. This interesting comparison confirms the role of modified structure and surface of MEPS in effectively reducing the amount of compressive strength loss in GLRPC despite its higher density compared to EPS. Table 5 also represents the reduction percentages in both dry density and compressive strength of GM-15 and mix No. 2 compared to the control mixture. As seen, with almost the same reduction in dry density, GM-15 exhibits a significantly lower reduction in compressive strength (between 17% and 20% depending on curing regime) than mix No. 2. This comparison confirms the better performance and the advantage of MEPS compared to EPS beads at the same condition. The satisfactory structural efficiency factor of mix GM-15 may

**Table 5.** Compressive strength and dry density reductions in GLRPCs

		Compressive strength reduction (%)		
Mix code	Dry density reduction (%)	28-day standard water curing	Heat curing at 200°C	
GM-15 No. 2	14.0% (1,875 kg/m <sup>3</sup> ) 16.0% (1,840 kg/m <sup>3</sup> )			

positively impact the engineering economics of the structures and their seismic resistance.

# Water Absorption

The permeation of water, ionic, and gaseous species is a key factor in the durability of cement-based composites. Concrete permeability is directly attributed to the porosity of its matrix microstructure (Hiremath and Yaragal 2018). It seems that the application of MEPS affects durability properties (like water absorption) of RPC, which has a dense inner structure because of its homogeneity. Therefore, it is important to study the water absorption behavior of GLRPC specimens, the effects of MEPS incorporation as paste replacement, and different curing conditions on water absorption of GLRPC mixes are displayed in Fig. 13. As a result, the water absorption slightly increases with increasing the MEPS replacement level, regardless of the curing conditions. The average value of water absorption for GLRPC under standard water curing conditions increased from 0.1644% for the control mix to 0.2042%, 0.2713%, and 0.3744% for replacement levels of 15%, 30%, and 45%, respectively. This is due to the hydrophobic nature of MEPS beads that entrap air bubbles into cement paste, which would increase the internal porosity and the water absorption of the concrete (Allahverdi et al. 2018; Sadrmomtazi et al. 2012). The results also show that the amount of water absorption increases with heat curing. The percentages of water absorption for mixes cured in the oven at 100°C, 150°C, and 200°C were about 0.7514%-1.7520%, depending on the replacement level. High-temperature curing will speed up the hydration progression of cement. This leads to the creation of relatively dense hydration product shells in the vicinity of the cement particles. Therefore, hydration products will not have enough opportunities to precipitate and diffuse in the interstitial space of cement particles. Thus, the outer product phase at a distance away from the cement particles becomes relatively porous (Edwin et al. 2017; Kjellsen 1996; Tam et al. 2010). Besides, in concrete cured at relatively high temperatures, the rapid temperature rise rate, differences in the thermal expansion coefficients of the solid phases of the concrete ingredients, and vapor pressure may lead to the propagation of microcracks that affect the concrete permeability (Abid et al. 2017; Sultan and Alyaseri 2020). It should also be noted that during heat curing of cement paste, densification of the calcium silicate hydrate (C-S-H) gel is associated with loss of C-S-H bound liquid water as well as increased polymerization of silicates. As a result, cement paste exhibits a coarse pore

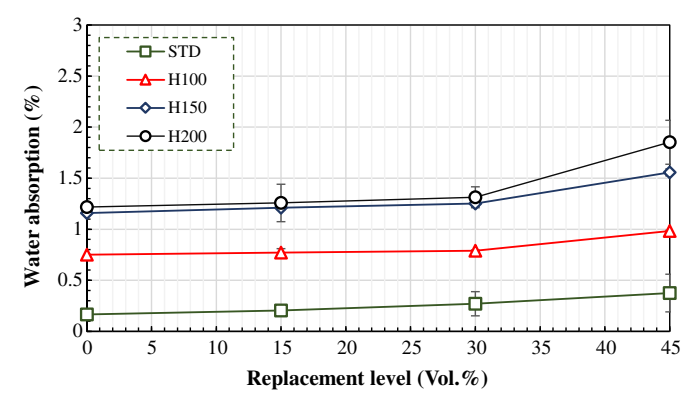
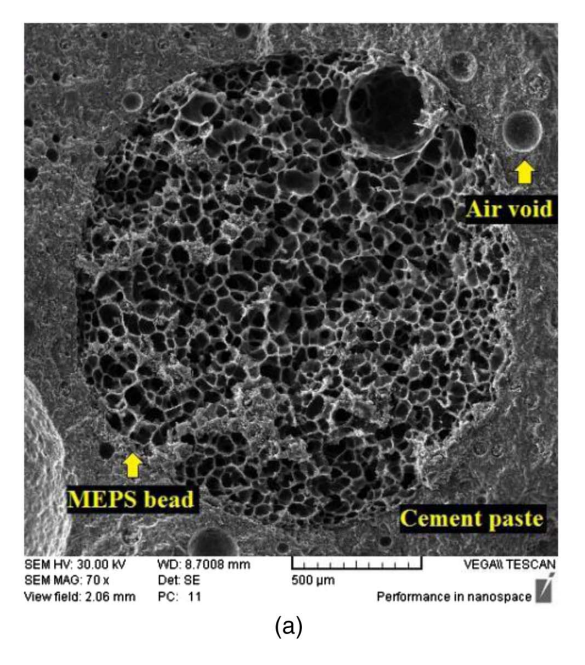


**Fig. 13.** Water absorption of the GLRPC specimens at different curing conditions (where STD = 28-day standard curing; H100 = heat curing at 100°C; H150 = heat curing at 150°C; and H200 = heat curing at 200°C).

structure with more capillary porosity (Thomas and Jennings 2002). The European Committee for Concrete–International Federation for Prestressing has classified the quality of concrete as good, average, and poor for water absorptions percentages of 0%–3%, 3%–5%, and above 5%, respectively. Accordingly, all GLRPC mixes studied in the present work can be considered as good quality concretes (CEB-FIP 1989; Nikbin et al. 2018), because their water absorption values are all less than 2%.

#### Microstructure

According to the microscale points of view, concrete mechanical and durability performances are directly influenced by aggregate characteristics, cement paste, and ITZ. Appreciable mechanical performance is achieved by higher ITZ densification, resulting in



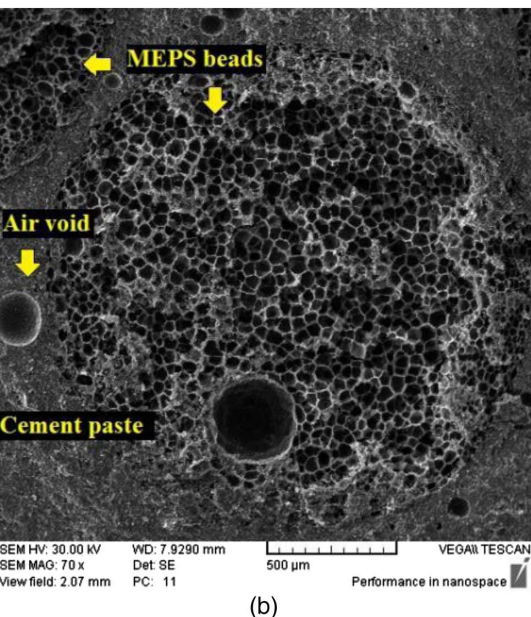


**Fig. 14.** Typical SEM micrographs from fracture surface of MEPS beads in GLRPC matrix: (a) 28-day standard water curing; and (b) 48-h heat curing at 100°C after 4 days of standard water curing.

the desired bond between cement paste and aggregate (Rossignolo et al. 2017).

Fig. 14 displays typical SEM micrographs prepared from the fracture surface of GLRPC with MEPS beads cured at different curing conditions, including 28-day standard water curing (A) and 4 days of standard water curing followed by 48 h of heat curing at 100°C. As seen independent of the curing conditions applied and despite the weak hydrophilic nature of MEPS, the GLRPC microstructure is very dense and uniform even in the ITZ, and there seems an excellent bonding between GLPRC paste and MEPS so that in many interfacial places, no transition zone can be observed. Entrapped air voids in the vicinity of the MEPS beads, however, are clearly visible. This excellent bonding between GLRPC paste and MEPS beads can be attributed to the nucleation seeding effect of SF. The incorporation of SF into the RPC mix results in uniform

hydration due to its essential role in the nucleation seeding for precipitation and growth of C-S-H. If SF particles are uniformly dispersed in the RPC mix, the nucleation seeding effect can result in uniform dispersion of C—S—H in the ITZ as well as in the matrix (Gutteridge and Dalziel 1990; Saikia and Brito 2012; Xue and Shinozuka 2013). Compared to the control mix (GM-0), the compressive strength loss in GLRPC mixtures incorporating MEPS is, therefore, mainly due to the very porous and soft structure of MEPS.

Microstructure analysis in the vicinity of the MEPS for specimens cured in the oven at 200°C showed that interconnection between cement matrix and MEPS has a high strength. At a temperature higher than 165°C the internal beehive structure of MEPS beads collapses toward the boundary layer and melts, subsequently in the form of hollow particles appear inside the RPC matrix.

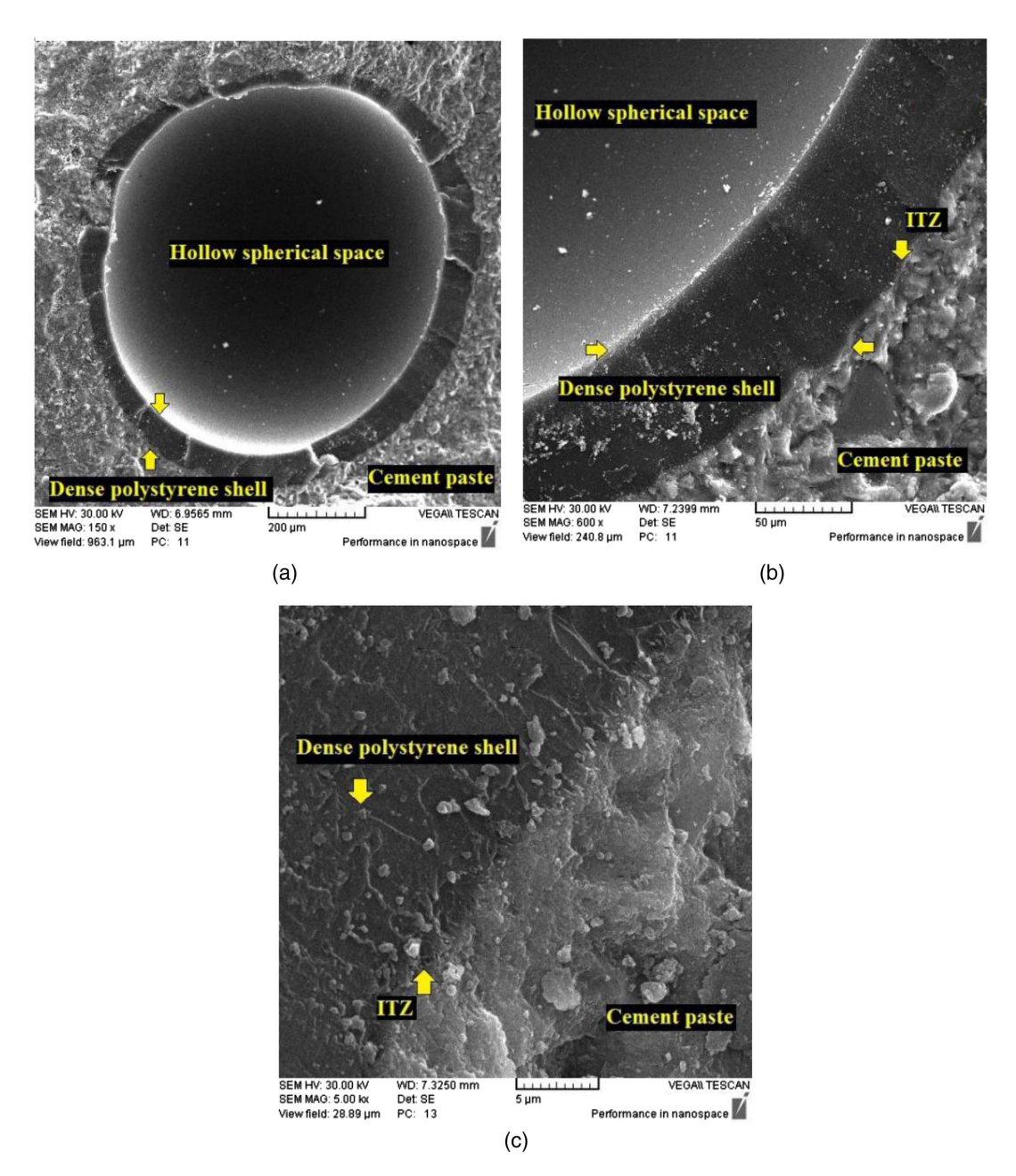


**Fig. 15.** Typical SEM micrographs from fracture surface of hollow spherical polystyrene beads in GLRPC matrix after 4 days of standard water curing followed by 48-h heat curing at 200°C: (a) polystyrene hollow bead in GLRPC matrix; and (b and c) ITZ between hollow spherical polystyrene bead and the cement paste.

These hollow particles have relatively spherical shapes and hard and stiff shells with a thickness of about 3%–10% original outer diameter. It is also observed at higher magnification power that the potent combinations between hollow spherical polystyrene beads and cement paste, and these combinations reflect sufficient Van der Waals forces at the interface. It seems that this new type of interconnection is characterized as one of the most appropriate of the plastic/cement-paste bond.

As observed in the section on the influence of curing temperature, a significantly higher compressive strength was achieved at higher heat curing temperatures. This significant compressive strength enhancement was related to the effect of heat curing temperature on the length of C-S-H chain, in addition to its significant effects on both rate and degree of progress of pozzolanic reactions between of calcium hydroxide and SF and also hydration reactions of GGBFS present in the cementitious system of RPC. SEM observations on fractured surfaces, however, revealed another critical and interesting cause for this observation. Fig. 15 shows typical SEM micrographs prepared from fracture surface of MEPS beads in GLRPC matrix after 4 days of standard water curing followed by 48-h heat curing at 200°C. As seen, curing at 200°C changed the structure and shape of MEPS beads into hollow spherical polystyrene beads of nonporous shells perfectly bonded to the GLRPC matrix. In fact, when EPS beads inside RPC matrix are heated to a temperature higher than 165°C, they undergo a structural collapse and start melting. The polystyrene melt then covers the surface of the cement paste in the empty spherical space with a thin layer. After cooling to temperatures lower than 165°C and solidification, the polystyrene melt forms a hollow sphere with a relatively hard and stiff shell that exhibits a very well bonding to the GLRPC matrix on its outer surface and shows no porosity and empty space in ITZ [as seen in Figs. 15(b and c)]. Therefore, compared to heat curing at 150°C, the positive microstructural changes happening in MEPS beads during heat curing at temperatures higher than the melting point of EPS can also contribute to compressive strength increase in GLRPC mixtures of the same replacement levels.

## **Conclusions**

The following conclusions are presented:

- 1. GLRPC with densities below 1,920 kg/m³ can be produced by incorporating thermally MEPS beads into green RPC. Replacement levels up to 30% of RPC paste volume by MEPS beads result in the development of high-strength lightweight concrete. Further replacement levels lead to lightweight concretes that drop into the structural class. Replacement levels exceeding 45% of RPC paste volume are not recommended due to large compressive strength reductions. GLRPC incorporating MEPS exhibits a significant structural efficiency that makes it viable as a sustainable structural lightweight material;
- Image analysis showed a relatively uniform distribution of MEPS beads inside the RPC matrix with minimum segregation without the utilization of any chemical surface modification agent;
- Enhanced mechanical properties of GLRPC incorporating MEPS, compared to GLRPC containing EPS, could be attributed to the dense microstructure of MEPS exhibiting a highly improved mechanical strength as well as an improved bonding between RPC paste and MEPS beads;
- 4. The water absorption of GLRPC slightly increases when incorporating MEPS aggregate at a higher replacement level. The curing temperature affects the amount of water adsorption more strongly so that water adsorption increases with increasing

- curing temperature. However, the relatively small value of water absorption for all the studied mixtures in this investigation remained less than 2%; and
- 5. Heat curing of GLRPC at 200°C changes the structure of MEPS beads and converts them into hollow spherical polystyrene beads with a relatively stiff and rigid shell. This, together with the effect of higher curing temperatures on hydration degree affect the mechanical properties of the GLRPC significantly. The enhanced compressive strength of GLRPC cured at 200°C, therefore, can be attributed to both the development of a denser RPC paste microstructure and the development of hollow spherical polystyrene beads resulting in an innovative high-tech plastic/cement-paste bonding.

Based on the results of the present study, the incorporation of MEPS into RPC and heat curing at 200°C after 4 days of standard water curing provide an effective way of producing a new lightweight cement-based composite exhibiting superior mechanical properties than GLRPC incorporating EPS beads. Future investigations are required to evaluate the durability performance of a composite structural material, which might provide opportunities to minimize the risk of the earthquake on concrete structures and probably other structural applications, e.g., offshore platforms, long-span bridges, and high-rise buildings, etc.

# **Data Availability Statement**

All data, models, and code generated or used during the study appear in the published article.

#### References

- Abid, M., X. Hou, W. Zheng, and R. Rizwan. 2017. "High temperature and residual properties of reactive powder concrete—A review." *Constr. Build. Mater.* 147 (519): 339–351. https://doi.org/10.1016/j.conbuildmat.2017.04.083.
- Ali, M. R., M. Maslehuddin, M. Shameem, and M. S. Barry. 2018. "Thermal-resistant lightweight concrete with polyethylene beads as coarse aggregates." *Constr. Build. Mater.* 164 (Mar): 739–749. https://doi.org/10.1016/j.conbuildmat.2018.01.012.
- Allahverdi, A., S. A. Azimi, and M. Alibabaie. 2018. "Development of multi-strength grade green lightweight reactive powder concrete using expanded polystyrene beads." *Constr. Build. Mater.* 172 (May): 457–467. https://doi.org/10.1016/j.conbuildmat.2018.03.260.
- Angelin, A. F., R. C. Lintz, W. R. Osório, and L. A. Gachet. 2020. "Evaluation of efficiency factor of a self-compacting lightweight concrete with rubber and expanded clay contents." *Constr. Build. Mater.* 257 (Oct): 119573. https://doi.org/10.1016/j.conbuildmat.2020.119573.
- Aslam, M., P. Shafigh, A. Nomeli, and M. Z. Jumaat. 2017. "Manufacturing of high-strength lightweight aggregate concrete using blended coarse lightweight aggregates." *J. Build. Eng.* 13 (Sep): 53–62. https://doi.org/10.1016/j.jobe.2017.07.002.
- Assaad, J. J., and A. El Mir. 2020. "Durability of polymer-modified lightweight flowable concrete made using expanded polystyrene." *Constr. Build. Mater.* 249 (Jul): 118764. https://doi.org/10.1016/j.conbuildmat.2020.118764.
- ASTM. 2005. Standard specification for silica fume used in cementitious mixtures. ASTM C1240. West Conshohocken, PA: ASTM.
- ASTM. 2012. Standard test method for compressive strength of cube concrete specimens. ASTM C109. West Conshohocken, PA: ASTM.
- ASTM. 2013a. Standard specification for chemical admixtures for concrete. ASTM C494. West Conshohocken, PA: ASTM.
- ASTM. 2013b. Standard test method for density, absorption, and voids in hardened concrete. ASTM C642-13. West Conshohocken, PA: ASTM.
  ASTM. 2017. Standard specification for Portland cement. ASTM C150. West Conshohocken, PA: ASTM.

- Aydin, S., H. Yazici, M. Y. Yardimci, and H. Yi. 2010. "Effect of aggregate type on mechanical properties of reactive powder concrete." ACI Mater. J. 107 (5): 441–449.
- Babu, K. G., and D. S. Babu. 2003. "Behaviour of lightweight expanded polystyrene concrete containing silica fume." Cem. Concr. Res. 33 (5): 755–762. https://doi.org/10.1016/S0008-8846(02)01055-4.
- Bonneau, O., V. Christian, M. Micheline, and A. Pierre-Claude. 2001. "Characterization of the granular packing and percolation threshold of reactive powder concrete." *Cem. Concr. Res.* 30 (12): 1861–1867. https://doi.org/10.1016/S0008-8846(00)00300-8.
- CEB-FIP (Comité Euro-International Du Béton). 1989. "Diagnosis and assessment of concrete structures: State-of-the-art report." CEB Bull 192 (2): 83–85.
- Cheah, C. B., L. L. Tiong, E. P. Ng, and C. W. Oo. 2019. "The engineering performance of concrete containing high volume of ground granulated blast furnace slag and pulverized fly ash with polycarboxylate-based superplasticizer." Constr. Build. Mater. 202 (Mar): 909–921. https://doi .org/10.1016/j.conbuildmat.2019.01.075.
- Chung, S. Y., M. Abd Elrahman, D. Stephan, and P. H. Kamm. 2018. "The influence of different concrete additions on the properties of lightweight concrete evaluated using experimental and numerical approaches." *Constr. Build. Mater.* 189 (Nov): 314–322. https://doi.org/10.1016/j .conbuildmat.2018.08.189.
- Costa, H., R. N. F. Carmo, and E. Júlio. 2018. "Influence of lightweight aggregates concrete on the bond strength of concrete-to-concrete interfaces." *Constr. Build. Mater.* 180 (Aug): 519–530. https://doi.org/10 .1016/j.conbuildmat.2018.06.011.
- Cwirzen, A., V. Penttala, and C. Vornanen. 2008. "Reactive powder based concretes: Mechanical properties, durability and hybrid use with OPC." Cem. Concr. Res. 38 (10): 1217–1226. https://doi.org/10.1016/j.cemconres.2008.03.013.
- Demirel, B., E. Gultekin, and K. E. Alyamac. 2019. "Performance of structural lightweight concrete containing metakaolin after elevated temperature." KSCE J. Civ. Eng. 23 (7): 2997–3004. https://doi.org/10.1007/s12205-019-1192-x.
- Edwin, R. S., E. Gruyaert, and N. De Belie. 2017. "Influence of intensive vacuum mixing and heat treatment on compressive strength and microstructure of reactive powder concrete incorporating secondary copper slag as supplementary cementitious material." Constr. Build. Mater. 155 (Nov): 400–412. https://doi.org/10.1016/j.conbuildmat.2017.08.036.
- Fashandi, H., H. R. Pakravan, and M. Latifi. 2020. "Application of modified carpet waste cuttings for production of eco-efficient lightweight concrete." *Constr. Build. Mater.* 198 (Feb): 629–637. https://doi.org/10.1016/j.conbuildmat.2018.11.163.
- Ganesh, P., and A. R. Murthy. 2019. "Tensile behaviour and durability aspects of sustainable ultra-high performance concrete incorporated with GGBS as cementitious material." *Constr. Build. Mater.* 197 (Feb): 667–680. https://doi.org/10.1016/j.conbuildmat.2018.11.240.
- Gökçe, H. S., S. Setenay, and A. Özge. 2017. "A new approach for production of reactive powder concrete: Lightweight reactive powder concrete (LRPC)." *Mater. Struct.* 50 (1): 58. https://doi.org/10.1617/s11527-016-0937-y.
- Gupta, T., S. Chaudhary, and R. K. Sharma. 2014. "Assessment of mechanical and durability properties of concrete containing waste rubber tire as fine aggregate." *Constr. Build. Mater.* 73 (Dec): 562–574. https://doi.org/10.1016/j.conbuildmat.2014.09.102.
- Gutteridge, W. A., and J. A. Dalziel. 1990. "Filler cement: The effect of the secondary component on the hydration of portland cement: Part I. A fine non-hydraulic filler." Cem. Concr. Res. 20 (5): 778–782. https://doi .org/10.1016/0008-8846(90)90011-L.
- Han, J., K. Wang, X. Wang, and P. J. M. Monteiro. 2016. "2D image analysis method for evaluating coarse aggregate characteristic and distribution in concrete." *Constr. Build. Mater.* 127 (Nov): 30–42. https://doi.org/10.1016/j.conbuildmat.2016.09.120.
- Hiremath, P. N., and S. C. Yaragal. 2017. "Effect of different curing regimes and durations on early strength development of reactive powder concrete." Constr. Build. Mater. 154 (Nov): 72–87. https://doi.org/10 .1016/j.conbuildmat.2017.07.181.

- Hiremath, P. N., and S. C. Yaragal. 2018. "Performance evaluation of reactive powder concrete with polypropylene fibers at elevated temperatures." *Constr. Build. Mater.* 169 (Apr): 499–512. https://doi.org/10 .1016/j.conbuildmat.2018.03.020.
- Kan, A., and R. Demirboğa. 2008. "A new technique of processing for waste-expanded polystyrene foams as aggregates." *J. Mater. Process. Technol.* 209 (6): 2994–3000. https://doi.org/10.1016/j.jmatprotec .2008.07.017.
- Khaloo, A. R., M. Dehestani, and P. Rahmatabadi. 2008. "Mechanical properties of concrete containing a high volume of tire—Rubber particles." Waste Manage. 28 (12): 2472–2482. https://doi.org/10.1016/j .wasman.2008.01.015.
- Kjellsen, K. O. 1996. "Heat curing and post-heat curing regimes of high-performance concrete: Influence on microstructure and CSH composition." Cem. Concr. Res. 26 (2): 295–307. https://doi.org/10.1016/0008-8846(95)00202-2.
- Maaroufi, M., K. Abahri, C. El Hachem, and R. Belarbi. 2018. "Characterization of EPS lightweight concrete microstructure by X-ray tomography with consideration of thermal variations." Constr. Build. Mater. 178 (Jul): 339–348. https://doi.org/10.1016/j.conbuildmat.2018.05.142.
- Majhi, R. K., A. N. Nayak, and B. B. Mukharjee. 2018. "Development of sustainable concrete using recycled coarse aggregate and ground granulated blast furnace slag." *Constr. Build. Mater.* 159 (Jan): 417–430. https://doi.org/10.1016/j.conbuildmat.2017.10.118.
- Mehta, S., S. Biederman, and S. Shivkumar. 1995. "Thermal degradation of foamed polystyrene." *J. Mater. Sci.* 30 (11): 2944–2949. https://doi.org /10.1007/BF00349667.
- Milling, A., A. Mwasha, and H. Martin. 2020. "Exploring the full replacement of cement with expanded polystyrene (EPS) waste in mortars used for masonry construction." *Constr. Build. Mater.* 253 (Aug): 119158. https://doi.org/10.1016/j.conbuildmat.2020.119158.
- Miskolczi, N., L. Bartha, and G. Dea. 2006. "Thermal degradation of polyethylene and polystyrene from the packaging industry over different catalysts into fuel-like feed stocks." *Polym. Degrad. Stab.* 91 (3): 517–526. https://doi.org/10.1016/j.polymdegradstab.2005.01.056.
- Neville, A. M. 1995. Properties of concrete. London: Longman.
- Nikbin, I. M., M. Aliaghazadeh, S. H. Charkhtab, and A. Fathollahpour. 2018. "Environmental impacts and mechanical properties of lightweight concrete containing bauxite residue (red mud)." *J. Cleaner Prod.* 172 (Jan): 2683–2694. https://doi.org/10.1016/j.jclepro.2017.11.143.
- Richard, P., and M. Cheyrezy. 1995. "Composition of reactive powder concretes." *Cem. Concr. Res.* 25 (7): 1501–1511. https://doi.org/10.1016/0008-8846(95)00144-2.
- Rossignolo, J. A., and M. V. Agnesini. 2002. "Mechanical properties of polymer-modified lightweight aggregate concrete." *Cem. Concr. Res.* 32 (3): 329–334. https://doi.org/10.1016/S0008-8846(01)00678-0.
- Rossignolo, J. A., M. S. Rodrigues, M. Frias, S. F. Santos, and H. S. Junior. 2017. "Improved interfacial transition zone between aggregatecementitious matrix by addition sugarcane industrial ash." *Cem. Concr. Compos.* 80 (Jul): 157–167. https://doi.org/10.1016/j.cemconcomp 2017.03.011
- Rumsys, D., E. Spudulis, B. Darius, and K. Gintaris. 2018. "Compressive strength and durability properties of structural lightweight concrete with fine expanded glass and/or clay aggregates." *Materials (Basel)* 11 (12): 2434. https://doi.org/10.3390/ma11122434.
- Sadrekarimi, A. 2004. "Development of a light weight reactive powder concrete." J. Adv. Concr. Technol. 2 (3): 409–417. https://doi.org/10 .3151/jact.2.409.
- Sadrmomtazi, A., J. Sobhani, M. A. Mirgozar, and M. Najimi. 2012. "Properties of multi-strength grade EPS concrete containing silica fume and rice husk ash." *Constr. Build. Mater.* 35 (Oct): 211–219. https://doi.org/10.1016/j.conbuildmat.2012.02.049.
- Saikia, N., and J. De Brito. 2012. "Use of plastic waste as aggregate in cement mortar and concrete preparation: A review." Constr. Build. Mater. 34 (Sep): 385–401. https://doi.org/10.1016/j.conbuildmat.2012 .02.066.
- Saikia, N., and J. De Brito. 2014. "Mechanical properties and abrasion behaviour of concrete containing shredded PET bottle waste as a partial

- substitution of natural aggregate." *Constr. Build. Mater.* 52 (Feb): 236–244. https://doi.org/10.1016/j.conbuildmat.2013.11.049.
- Sayadi, A. A., J. V. Tapia, T. R. Neitzert, and G. C. Clifton. 2016. "Effects of expanded polystyrene (EPS) particles on fire resistance, thermal conductivity and compressive strength of foamed concrete." Constr. Build. Mater. 112 (Jun): 716–724. https://doi.org/10.1016/j.conbuildmat.2016 .02.218.
- Shafigh, P., M. Z. Jumaat, and H. Mahmud. 2011. "Oil palm shell as a lightweight aggregate for production high strength lightweight concrete." Constr. Build. Mater. 25 (4): 1848–1853. https://doi.org/10.1016 /j.conbuildmat.2010.11.075.
- Shafigh, P., M. Z. Jumaat, H. B. Mahmud, and U. J. Alengaram. 2013. "Oil palm shell lightweight concrete containing high volume ground granulated blast furnace slag." Constr. Build. Mater. 40 (Mar): 231–238. https://doi.org/10.1016/j.conbuildmat.2012.10.007.
- Shen, P., L. Lu, Y. He, F. Wang, and S. Hu. 2019. "Cement and concrete research the effect of curing regimes on the mechanical properties, nano-mechanical properties and microstructure of ultra-high performance concrete." Cem. Concr. Res. 118 (Apr): 1–13. https://doi.org/10 .1016/j.cemconres.2019.01.004.
- Sultan, H. K., and I. Alyaseri. 2020. "Effects of elevated temperatures on mechanical properties of reactive powder concrete elements." *Constr. Build. Mater.* 261 (Nov): 120555. https://doi.org/10.1016/j.conbuildmat.2020.120555.
- Tam, C. M., V. W. Y. Tam, and K. M. Ng. 2010. "Optimal conditions for producing reactive powder concrete." *Mag. Concr. Res.* 62 (10): 701–716. https://doi.org/10.1680/macr.2010.62.10.701.
- Thomas, J. J., and H. M. Jennings. 2002. "Effect of heat treatment on the pore structure and drying shrinkage behavior of hydrated cement paste." *J. Am. Ceram. Soc.* 85 (9): 2293–2298. https://doi.org/10.1111/j.1151 -2916.2002.tb00450.x.
- Vigneshwari, M., K. Arunachalam, and A. Angayarkanni. 2018. "Replacement of silica fume with thermally treated rice husk ash in reactive powder concrete." *J. Cleaner Prod.* 188 (Jul): 264–277. https://doi.org/10.1016/j.jclepro.2018.04.008.
- Wu, F., C. Liu, W. Sun, Y. Ma, and L. Zhang. 2019a. "Effect of peach shell as lightweight aggregate on mechanics and creep properties of concrete." Eur. J. Environ. Civ. Eng. 24 (14): 2534–2552. https://doi.org/10.1080/19648189.2018.1515667.
- Wu, F., C. Liu, L. Zhang, Y. Lu, and Y. Ma. 2018. "Comparative study of carbonized peach shell and carbonized apricot shell to improve the performance of lightweight concrete." *Constr. Build. Mater.* 188 (Nov): 758–771. https://doi.org/10.1016/j.conbuildmat.2018.08.094.

- Wu, H., and P. Sun. 2007. "New building materials from fly ash-based lightweight inorganic polymer." *Constr. Build. Mater.* 21 (1): 211–217. https://doi.org/10.1016/j.conbuildmat.2005.06.052.
- Wu, T., X. Yang, H. Wei, and X. Liu. 2019b. "Mechanical properties and microstructure of lightweight aggregate concrete with and without fibers." *Constr. Build. Mater.* 199 (Feb): 526–539. https://doi.org/10 .1016/j.conbuildmat.2018.12.037.
- Xue, J., and M. Shinozuka. 2013. "Rubberized concrete: A green structural material with enhanced energy-dissipation capability." *Constr. Build. Mater.* 42 (May): 196–204. https://doi.org/10.1016/j.conbuildmat.2013.01.005.
- Xun, X., Z. Ronghua, and L. Yinghu. 2020. "Influence of curing regime on properties of reactive powder concrete containing waste steel fibers." *Constr. Build. Mater.* 232 (Jan): 117129. https://doi.org/10.1016/j .conbuildmat.2019.117129.
- Yanzhou, P., J. Zhang, J. Liu, J. Ke, and F. Wang. 2015. "Properties and microstructure of reactive powder concrete having a high content of phosphorous slag powder and silica fume." *Constr. Build. Mater.* 101 (Part 1): 482–487. https://doi.org/10.1016/j.conbuildmat.2015 .10.046.
- Yazıcı, H., M. Y. H. Yardımcı, S. A. Yiğiter, and T. Selçuk. 2010. "Mechanical properties of reactive powder concrete containing high volumes of ground granulated blast furnace slag." Cem. Concr. Compos. 32 (8): 639–648. https://doi.org/10.1016/j.cemconcomp.2010.07.005.
- Yazıcı, H., H. Yig, A. S. Karabulut, and B. Baradan. 2008. "Utilization of fly ash and ground granulated blast furnace slag as an alternative silica source in reactive powder concrete." Fuel 87 (12): 2401–2407. https:// doi.org/10.1016/j.fuel.2008.03.005.
- Yu, Q. L., P. Spiesz, and H. J. H. Brouwers. 2013. "Development of cement-based lightweight composites: Part 1: Mix design methodology and hardened properties." *Cem. Concr. Compos.* 44 (Nov): 17–29. https://doi.org/10.1016/j.cemconcomp.2013.03.030.
- Záleská, M., M. Pavlíková, J. Pokorny, O. Jankovský, Z. Pavlík, and R. Černý. 2018. "Structural, mechanical and hygrothermal properties of lightweight concrete based on the application of waste plastics." Constr. Build. Mater. 180 (Aug): 1–11. https://doi.org/10.1016/j.conbuildmat. 2018.05.250.
- Zanni, H., M. Cheyrezy, V. Maret, S. Philippot, and P. Nieto. 1996. "Investigation of hydration and pozzolanic reaction in reactive powder concrete (RPC) using 29 Si NMR." Cem. Concr. Res. 26 (1): 93–100. https://doi.org/10.1016/0008-8846(95)00197-2.